HHS Public Access

Author manuscript

Biomaterials. Author manuscript; available in PMC 2015 July 06.

Published in final edited form as:

Biomaterials. 2011 August ; 32(23): 5320–5329. doi:10.1016/j.biomaterials.2011.04.025.

A 3D aligned microfibrous myocardial tissue construct cultured under transient perfusion

Halime Kenar[a,b,1], **Gamze T. Kose**[b,c], **Mehmet Toner**[d], **David L. Kaplan**[e], and **Vasif Hasirci**[a,b,*]

[a]BIOMAT, Dept. of Biological Sciences, Biotechnology Research Unit, Middle East Technical University, Ankara 06531, Turkey

[b]BIOMATEN Center of Excellence in Biomaterials and Tissue Engineering, METU, Biotechnology Research Unit, Ankara 06531, Turkey

[c]Department of Genetics and Bioengineering, Yeditepe University, Istanbul 34755, Turkey

[d]Surgical Services and Center for Engineering in Medicine, Massachusetts General Hospital, Harvard Medical School and Shriners Hospital for Children, Boston, MA 02114, USA

[e]Department of Biomedical Engineering, Bioengineering & Biotechnology Center, Tufts University, 4 Colby Street, Medford, MA 02155, USA

Abstract

The goal of this study was to design and develop a myocardial patch to use in the repair of myocardial infarctions or to slow down tissue damage and improve long-term heart function. The basic 3D construct design involved two biodegradable macroporous tubes, to allow transport of growth media to the cells within the construct, and cell seeded, aligned fiber mats wrapped around them. The microfibrous mat housed mesenchymal stem cells (MSCs) from human umbilical cord matrix (Wharton's Jelly) aligned in parallel to each other in a similar way to cell organization in native myocardium. Aligned micron-sized fiber mats were obtained by electrospinning a polyester blend (PHBV (5% HV), P(L-D,L)LA (70:30) and poly(glycerol sebacate) (PGS)). The micron-sized electrospun parallel fibers were effective in Wharton's Jelly (WJ) MSCs alignment and the cells were able to retract the mat. The 3D construct was cultured in a microbioreactor by perfusing the growth media transiently through the macroporous tubing for two weeks and examined by fluorescence microscopy for cell distribution and preservation of alignment. The fluorescence images of thin sections of 3D constructs from static and perfused cultures confirmed enhanced cell viability, uniform cell distribution and alignment due to nutrient provision from inside the 3D structure.

Keywords

Cardiac tissue engineering; Stem cell; Cell morphology; Polyhydroxybutyric acid; Polylactic acid; DMA (dynamic mechanical analysis)

[*]Corresponding author. Tel.: +90 312 2105180; fax: +90 312 2101542. vhasirci@metu.edu.tr (V. Hasirci).

[1]Present address: Kocaeli University, Center for Stem Cell and Gene Therapies Research and Practice, 41380 Izmit/Kocaeli, Turkey.

1. Introduction

With progress in scaffold development technology, the field of tissue engineering is advancing toward the generation of tissue substitutes, which better mimic the complexity of the natural tissues. The availability of materials and processing techniques suitable for the construction of tissue substitutes with unique mechanical properties and complex structures is opening the door for functional tissue replacements. It is now more evident that the microenvironment where the cells reside is very influential in controlling cellular behavior, which in turn is reflected in engineered functionality. The mesenchymal stem cells (MSCs), which are increasingly utilized in tissue engineering applications due to their pluripotency, are highly sensitive to the chemical, mechanical and structural properties of the scaffolds they are grown on [1–3].

With the realization of this fact, many investigators have been modifying polymer bulk properties through blending of existing polymers or synthesis of new polymers. Also increasing efforts are being spent on introducing structural complexity to the scaffolds as MSCs behave differently in two and three-dimensional (3D) environments [4,5]. In the past decade, electrospinning has gained popularity over simpler solvent casting and particulate leaching techniques in the creation of a more natural 3D microenvironment for the cells. Electrospinning enables the fabrication of highly porous scaffolds with extensively interconnected pores which allow cell-to-cell contact, migration in all directions, transportation of nutrients and metabolites, and encourage blood vessel formation; all of these combined help cell survival and proliferation. The fibrous scaffolds obtained through electrospinning have a size scale and architecture similar to those of the native extracellular matrix and are very useful especially in introducing anisotropy, particularly important in mimicking aligned fibrous tissues like myocardium, skeletal muscle, tendon, ligament and meniscus [6,7].

Both the architecture of native myocardium and its cardiomyocyte arrangement which enable a forceful syncytial contraction point out the necessity to align cardiomyocytes in the 3D cell carrier. This necessity was supported by an *in vitro* study; a comparative study carried out on cardiomyocyte function on electrospun random and aligned polymer fibers showed that cellular alignment enhanced cardiomyocyte maturation [8]. Structural resemblance and uniaxial cellular alignment can be achieved effectively on aligned fibers, although some problems, like difficulty in cell penetration [9,10] and obtaining sufficiently thick constructs especially from nanofibrous scaffolds, still prevail. Several methods, such as culturing cell seeded scaffolds in an orbital shaker or under perfusion, were proposed to promote cell penetration and homogeneity and to maintain cell viability in thick scaffolds [11,12]. Neonatal rat cardiomyocytes expressing sarcomeric α-actin were relatively uniformly distributed throughout 1.5 mm-thick spongy constructs seeded and cultivated in perfusion but confined within only a 200–300 μm thick top layer of constructs seeded and cultivated in orbitally mixed dishes for 7 days [11]. It was reported that it takes at least 6 weeks of culture in an orbital shaker for full occupancy of 0.75 mm thick aligned mesh of nanofibrous poly(ε-caprolactone) by mesenchymal stem cells [12]. In comparison with the irreplaceable effect of perfusion in obtaining a uniform cell distribution and viability in thick scaffolds, it was reported for constructs cultured with interstitial flow of medium that most

of the cells exhibited rounded morphology owing to direct exposure to hydrodynamic shear stress [13]. The introduction of a separate channel compartment for medium flow significantly improved metabolic activity and viability of cardiac cells [14], and in another study introduction of a parallel channel array to the scaffold improved cell morphology, where most cardiomyocytes had elongated shapes [15,16]. In the native myocardium, blood is confined within the capillary bed and is not in direct contact with cardiac cells, avoiding any possibility of damage by hydrodynamic shear stress.

Previously, we had reported on the production of aligned fibrous scaffolds with fiber density suitable for cell penetration by using a special frame collector [17]. At least 8–9 Wharton's Jelly MSC layers with their nuclei and cytoskeleton aligned were achieved with a single mat. A method of rolling the mats around macroporous biodegradable tubing was proposed to obtain homogeneous constructs. A biomimetic approach was applied by introducing macroporous tubing to serve as separate compartments for medium flow, in order to prevent cell damage through hydrodynamic shear stress. The present study describes a method to preserve the viability of the cells, maintain their anisotropy and establish an interlayer contact in the multilayered construct during the extended *in vitro* culture. The 3D construct was integrated into a home-made microbioreactor through biodegradable tubing to provide fresh medium to the cells residing within the mats. The 3D construct was cultured for two weeks in this microbioreactor while perfusing a cardiomyogenic medium through the macroporous tubing. Subsequently, the construct was analyzed for cell distribution and maintenance of alignment by fluorescence microscopy, and for cardiomyogenic marker expression by RT-PCR and immunocytochemistry.

2. Materials and methods

2.1. Synthesis and characterization of poly(glycerol sebacate)

Poly(glycerol sebacate) was synthesized using a procedure by Wang et al. [18]. A 250 mL three-neck flask equipped with a N_2 inlet, and thermometer adapter was charged with anhydrous glycerol and sebacic acid (1:1 mol ratio). N_2 was bubbled through the mixture while it was heated to 120 °C with constant stirring for 24 h, before the N_2 was disconnected. The flask was then connected to a vacuum line and the reaction was continued at 120 °C for another 24 h. PGS prepolymer molecular weight was determined by Gel Permeation Chromatography (Polymer Laboratories (UK), PL-GPC 220 column) at a flow rate of 1 mL/min at 30 °C. The Polystyrene Universal Calibration method was used for determination of the molecular weight.

2.2. Preparation of aligned microfiber mats through electrospinning

Poly(3-hydroxybutyrate-co-3-hydroxyvalerate) (PHBV, MW 222.2 kDa, containing 5% 3-hydroxyvalerate, Sigma–Aldrich Co., USA), P(L-D,L)LA (70:30, i.v. 5.5–6.5 dL/g, Boehringer-Ingelheim, Germany), and poly(glycerol sebacate) (PGS) (synthesized above, MW 9929 Da, polydispersity 1.8) were blended by dissolving in chloroform (Chl) : N,N-dimethyl formamide (DMF) (95:5 v/v). PHBV:P(L-D,L)LA solution (1:1 w/w, 5%) that contained 0, 1, 2, or 4% w/w PGS in Chl:DMF (95:5) was electrospun at a flow rate of 30

μL/min at 18 kV potential from a 24 cm distance between the needle tip and the receiver metal frame.

The home-made electrospinning set up used in this study consisted of a high voltage supply (Gamma High Voltage Research, Ormond Beach, FL, USA), a syringe pump (New Era Pump Systems, NE 1800), a 10 mL syringe capped with a blunt end-needle, and a grounded metal frame collector. The conditions were optimized to have minimum fiber fusion and minimum bead formation.

Dynamic mechanical analysis (DMA) of the aligned microfiber mats with 0 or 2% w/w PGS were performed with a Perkin Elmer Pyris Diamond DMA (USA) viscoelastic analyzer. Temperature scans at a 1, 2 and 4-Hz frequencies were carried out. The samples were tested at temperature range of −50 °C–100 °C at a heating rate of 3 °C min^{-1} under nitrogen atmosphere. The analysis was carried out under oscillatory tension mode. The storage modulus (E′), loss modulus (E″) and tan δ values were recorded against temperature at different frequencies. The T_g was evaluated from the peak position of the tan δ (E″/E′) versus temperature curve.

2.3. Preparation of macroporous biodegradable tubing

For the preparation of a bifunctional tubing with nonporous and macroporous regions, a 96:4 (w/w) blend of P(L-D,L)LA with PGS was first prepared in chloroform (2% solution) and applied on a 2 cm section of a stainless steel wire (dia 0.5 mm) by dipping for 10 s and drying in the hood. This process was repeated 6 times. The P(LD, L)LA-PGS (96:4 w/w, 3.5%) solution was prepared in dioxane and coated on the remaining untreated part of the stainless steel wire by dipping for 10 s and subsequently freezing at −80 °C and lyophilizing to obtain a macroporous coat with a closed end. The resulting biodegradable tubing was removed from the wire in water and studied under stereomicroscope (Nikon SMZ 1500) and with scanning electron microscope (QUANTA 400F Field Emission SEM).

2.4. Preparation of the microbioreactor

A poly(dimethyl siloxane) (PDMS) chamber with 1 × 4.5 × 1 cm^3 volume was prepared by using a PMMA mold. The PMMA mold was immersed in PDMS prepolymer-catalyst mixture (in a 10:1 w/w ratio, Sylgard 184 Elastomer Kit, Dow Corning, USA) and PDMS was polymerized at 60 °C for 3 h. The resulting PDMS chamber was removed, two inlets and one outlet were drilled through its wall and Tygon tubing inserted for medium transport through the chamber.

2.5. hWJ MSC isolation from umbilical cord matrix and culture

Human Wharton's Jelly MSCs (WJ MSCs) were isolated from umbilical cord matrix. Umbilical cords were collected from full-term births with informed consent of the mothers after either caesarean section or normal delivery and aseptically stored at 4 °C in sterile saline until processing. The interval between collection and isolation of WJ MSCs was at most 24 h. To isolate WJ MSCs, the cords were rinsed several times with sterile saline and cut into 2–4 cm long segments, the vessels were stripped manually and the walls were cut open. The explants were transferred to 6- well plates containing αMEM/Ham F-12 (1:1)

with 2% fetal bovine serum, 100 U/mL penicillin and 100 μg/mL streptomycin. They were left undisturbed for 2 weeks to allow migration of cells from the explants. WJ MSCs were subcultured, grown using the same media and cryopreserved at passages 1 and 2. The mesenchymal origin of the cells was shown by osteoblastic and chondrogenic differentiation as stated previously [17].

2.6. hWJ MSC proliferation on the aligned microfiber mats

Upon obtaining confluent monolayers, third passage WJ MSCs were detached from the flask surface, resuspended in αMEM/Ham F-12 (1:1) with 10% FCS, 1% nonessential amino acids and 100 U/mL penicillin and 100 μg/mL streptomycin, and 3×10^4 cells were seeded on PHBV:P(L-D,L)LA and PHBV:P(L-D,L)LA:PGS (with 1, 2 and 4% PGS) aligned fiber mats with 1×1 cm^2 area that were either unmodified or modified via collagen type I adsorption (from 40 μg/mL collagen solution). Cell seeded mats were incubated at 37 °C in the CO_2 incubator for 1 and 14 days and cell number on the mats was determined with MTS test at these time points. Briefly the mats were transferred into freshly prepared 500 μL of low Glc DMEM with 10% FBS and 10% MTS/PES, in a new 24-well plate and the plate was incubated at 37 °C in the CO_2 incubator for 2 h, and finally 200 μL aliquots were taken from the wells and absorbance was determined at 490 nm using an Elisa Plate Reader (Molecular Devices (USA), Model Maxline). Cell numbers were calculated using a calibration curve that was prepared using the same protocol.

2.7. Assembly and characterization of 3D constructs

Electrospun aligned fiber mats of PHBV:P(L-D,L)LA:PGS (49:49:2) were seeded with undifferentiated WJ cells, cultured for 14 days and then rolled around the macroporous region of the biodegradable tubing to obtain the 3D construct. The system was designed to be able to send the cell growth medium through the tubing to the cells located deep within the layers of the mats.

The mats (3.5×6 cm^2) were placed in sterile petri plates of 10 cm diameter, sterilized under UV light (UV C, 15 min each side), treated with collagen Type I (40 μg/mL collagen solution transferred on mats for 10 min and mats dried after collagen solution removal) and seeded with 3×10^5 WJ MSC cells (from 2×10^5 cells/ mL cell suspension) and cultured for 14 days in the medium (αMEM/Ham F-12 (1:1) with 10% fetal bovine serum, 1% non-essential amino acids, and 100 U/mL penicillin and 100 μg/mL streptomycin) under static conditions in the CO_2 incubator (SANYO MCO-17 AIC, Sanyo Electric Co. Ltd., Japan, 5% CO_2, 37 °C). The medium was refreshed twice a week. Representative samples were fixed in formaldehyde (4%) for 30 min at room temperature (RT), and the cells were then permeabilized by treating with 0.1% Triton X-100 for 5 min at RT. Non-specific binding was blocked by incubating in 1% BSA at 37 °C for 30 min. The samples were stained with FITC-labeled Phalloidin (1:100 dilution in 0.1% BSA from stock solution of 0.1 mg/mL FITC-Phalloidin, Sigma Aldrich Co., USA) to observe the actin cytoskeleton and with propidium iodide (PI) solution (10 min, RT) for the nuclei. After washing with PBS, the samples were transferred to microscope slides and observed using a CLSM (Leica DM 2500, Germany) at 488 nm for Phalloidin and 532 nm for PI.

Collagen Type I gel was layed on the aligned fiber mats on which WJ MSCs had grown for 14 days and then the mats rolled around the macroporous portion of sterile biodegradable tubes to form a 3D construct where the fibers were parallel to the main axis of the tubing. Collagen Type I gel was used to keep the mat layers closer and connected to each other and prevent unwinding after 3D construct formation. One half-length mat was rolled around one tubing, another full-length mat was half rolled around another tubing and both tubing brought together by rolling the remaining part of the mat around both. For SEM analysis, the constructs were washed with distilled water, frozen at −80 °C and gross-sectioned with a scalpel in their frozen state. Then the sections were dried at room temperature and were coated with Cd–Au to examine with SEM.

2.8. Culture in the microbioreactor

To assemble the 3D construct in the microbioreactor, the PDMS chamber and a glass cover were sterilized under UV C for 15 min. Tygon tubes (Small Parts, Tygon Micro Bore PVC Tubing) were sterilized by flushing with 70% EtOH and inserted in the inlet and outlet holes drilled through the PDMS chamber walls. The 3D constructs were placed in the PDMS chambers that were full of media. For the dynamic case the medium was perfused through the biodegradable tubes, whose nonporous portions were inserted to the inner side of the chamber inlets to become connected to the tygon tubes through the PDMS wall (Fig. 1), while in the static case there was no flow. Cardiac differentiation medium DMEM high Glc with 10% FCS, 1% non-essential amino acids, 1% Pen-Strep, 100 μg/mL bovine insulin (Sigma), 1 ng/mL IL 1β (Biosource) and 2 mM valproic acid (Sigma) was applied to the 3D constructs in the static and perfused cultures for 14 days. The medium in the chambers was refreshed every third day. A total of 250 μL medium was perfused trough the 3D construct in the perfused chamber using a syringe pump (New Era Pump Systems, NE 1800) at a rate of 100 μL/h every third day. Both constructs were cultured for 14 days.

2.9. Analysis of the 3D constructs cultured in the microbioreactor

After 14 days of culture both constructs were cut with a scalpel into 1 cm-long pieces. One of the pieces was transferred into a cell lysis buffer for further RNA isolation and RT-PCR analysis. Cardiac specific gene expression of the cells in both cultures was analyzed with RT-PCR. Total RNA was isolated from WJ MSCs exposed to cardiac differentiation factors using Qiagen RNeasy Kit according to manufacturer's instructions and stored at −80 °C. The cDNA was synthesized, and then amplified with PCR using OneStep RT-PCR kit (RobusT II, Finnzymes). PCR was performed in a 20 μL reaction solution with 2.5 mM $MgCl_2$ for Nkx 2.5 and 1.5mM for all other genes. The RT-PCR conditions were as follows: 45 min at 48 °C, 2 min at 94 °C followed by 30 cycles of 94 °C for 30 s, 55 °C for 30 s, and 72 °C for 1 min, and final extension for 10 min at 72 °C. Amount of the template RNA used was 30 ng/ reaction. Primer sequences (forward, reverse) and lengths of the amplified products are given in Table 1. β-Actin was analyzed as a housekeeping gene. The PCR products were size fractionated by 2% agarose gel electrophoresis, stained with ethidium bromide, and visualized by UV illumination.

Another piece of 3D construct was embedded in OCT (Tissue-Tek® O.C.T. Compound) for cryosectioning prior to immunostaining. The 20 μm thick longitudinal sections of the

engineered tissues, obtained by cryosectioning, were immunostained for ventricular α/β MHC (Chemicon) for evaluation of cardiomyogenic differentiation and stained with FITC-Phalloidin for evaluation of cell alignment and density. The fixed cells were rinsed 3 times with PBS and incubated in 100 mM glycine for 15 min (to saturate reactive PFA groups). The samples were washed again 3 times with PBS and incubated in 0.1% Triton X-100 for 10 min. After rinsing 3 times with PBS the background was blocked with 1% BSA solution at 37 °C for 30 min. Next, the samples were left for 1 h in the 0.1% BSA solution that contained the primary antibody for α/β MHC (1:10 dilution) at 37 °C. The cells were washed 3 times with PBS and incubated with the secondary antibody (Alexa Fluor 532 labeled, 1:100 in PBS) for 1 h at 37 °C. After rinsing 3 times with PBS, and counterstaining cell nuclei with DAPI, the samples were observed under the confocal microscope (Leica DM 2500, Germany).

2.10. Statistical analysis

Statistical analysis of data for cell proliferation was carried out by one-way analysis of variance (ANOVA), followed by Tukey's test for multiple comparisons to determine the values that were significantly different. Differences were considered statistically significant at $p < 0.05$.

3. Results

3.1. Aligned microfiber mats prepared through electrospinning

Biodegradable polyesters like P(L-D,L)LA and PHBV are biocompatible polymers widely used as biomaterials and in tissue engineering. However, their hydrophobicity and rigidity are generally a disadvantage. It is necessary to have polymers with higher flexibility especially in the engineering of soft tissues, like heart, where the cardiac cells need to flex and contract to function properly. PGS, being a hydrophilic and low molecular weight polymer, was blended with these polymers to augment their hydrophilicity and flexibility through plasticizing, in order to improve cell attachment and especially make the scaffold suitable for contractions.

PHBV:P(L-D,L)LA:PGS (PPG) blends were used to obtain micron-size aligned fiber mats, through electrospinning (Fig. 2). PHBV:P(LD, L)LA solution (1:1 w/w, 5%) with varying concentrations of PGS (0, 1, 2 or 4% w/w PGS) in Chl:DMF of 95:5 volumetric ratio was electrospun with an expectation to obtain more flexible mats with increase in PGS concentration. Fiber diameters in the range of 1.16–1.37 μm were obtained.

Increase in PGS content in the polymer blend did not cause a significant change in fiber diameter, however, as PGS content increased to 4%, fiber fusions increased. Orientation of the fibers parallel to each other was more pronounced in the initial layers of the mat and this decreased as the mats became thicker. Mats with 12 ± 3 μm thickness were obtained.

3.2. DMA analysis of the mats

For most viscoelastic materials, the storage modulus (measured in tension) is similar to the Young's modulus, as measured by nonoscillatory mechanical tests. The loss modulus is

proportional to the heat dissipated per cycle as a result of molecular motion. Tangent delta, the damping term, represents the ratio of energy dissipated to the energy stored during one oscillation cycle. The DMA data of aligned fiber mats (Table 2) revealed an increase in storage modulus of PHBV:P(L-D,L)LA (PP) upon addition of 2% PGS, in contrast to our expectations, resulting in a more reinforced material. At 1 and 2 Hz frequencies, which represent the physiological frequency interval of beating heart, no change in storage modulus of PP and decrease in storage modulus of PHBV:P(L-D,L)LA:PGS (49:49:2) (PPG2)with increase in temperature from 25 °C (room temperature) to 37 °C (body temperature) were observed. An increase in loss modulus was observed for both mat types. At 4 Hz frequency the same trend was preserved for storage modulus of PPG2, while the storage modulus of PP increased. Loss modulus of PPG2 stayed constant independent of temperature at 4 Hz frequency. A single T_g value (the maximum value obtained from Tangent delta peaks) was obtained for the PP blend, indicating a thermodynamic miscibility, i.e. a single homogeneous phase, while two T_g values (an additional small peak in Tangent delta curve) were obtained upon addition of PGS to this blend. The T_g values increased as the frequency increased from 1 Hz to 4 Hz, since at higher frequencies there is insufficient time for chain uncoiling to occur and the material becomes relatively stiff. From the table it can be seen that Tangent delta, i.e. damping, increases with increase in temperature and frequency applied, and the values are higher for the PP blend.

3.3. The macroporous biodegradable tubing (hollow fibers)

Hybrid tubing of P(L-D,L)LA-PGS with both nonporous and macroporous regions were obtained by dip coating one end of a stainless steel wire (dia: 0.5 mm) in a solution of the polymer in chloroform at room temperature, and after drying, by dip coating the uncoated region in a polymer solution in dioxane, and drying by lyophilization. Stereomicrographs of the polymeric tubes, which had both nonporous and closed-end macroporous regions, were obtained (Fig. 3). The cross section of the tubing wall examined with SEM revealed the interconnectivity of the porous structure and the uniform central hole (Fig. 3d).

3.4. The 3D construct

To assemble a 3D construct, two aligned fiber mats with WJ MSCs grown on them for 14 days were wrapped around the permeable parts of two biodegradable tubes, so that the fibers are parallel to each other and to the longitudinal axis of the tubes (Fig. 4).

3.5. In vitro performance on the mats

3.5.1. hWJ MSC proliferation on the aligned microfiber mats—Electrospun aligned fiber mats of PP and PPG blends (1 × 1 cm^2) were seeded with WJ MSCs and then incubated for 1 and 14 days at 37 °C in the CO_2 incubator (5% CO_2), to study the effect of chemical property of mats on cell proliferation. MTS assay was carried out after 24 h of cell seeding, to determine the number of cells attached on each sample. No significant difference could be observed in terms of cell attachment on PPG blend mats, which contained 1, 2 or 4% PGS, although the mats with 2 or 4% PGS performed better (Fig. 5a). The presence of adsorbed collagen on the mats caused a significant improvement in cell attachment.

Further cell proliferation experiments were done with PP and PPG2 mats. Cell attachment on the TCPS was found to be the highest, followed by collagen adsorbed mats, especially the collagen adsorbed PP mats (Fig. 5b). Type I collagen is found in the ECM of many tissue types in the body, including cardiac tissue and bears the RGD (arginine–glycine–aspartic acid) amino acid sequence, an attachment site for integrins that anchor the cell to a surface. Presence of collagen on the surface improved cell attachment to the mats. In the absence of collagen, there was no significant difference in the cell attachment on PP and PPG2 mats, that is presence of 2% PGS in the polymer blend did not lead to a significant change in cell attachment.

The highest cell proliferation rate and the lowest standard deviation within 14 days were obtained on the PPG2 mats, when compared to the PP and TCPS surfaces. A reasonable explanation for this behavior could be that cells can penetrate easily within the mat through the voids among the aligned fibers, therefore the mats should be considered as 3D scaffolds as opposed to 2D surface of TCPS. Presence of collagen on both types of mats significantly decreased the cell proliferation rate. RGD-integrin association is known to affect cell proliferation and/or differentiation [19], and it is seen from Fig. 5b that Type I collagen slows down the proliferation of WJ MSCs.

A significant difference in proliferation rate was observed between PP and PPG2 mats, which points to the positive effect of more hydrophilic material on cell proliferation, either by improving cell-material interaction or cell penetration into the mat, or both. Therefore, the presence of PGS in the bulk material, even a low amount, promoted cell proliferation.

3.5.2. hWJ MSC penetration into the aligned microfiber mats—The ultimate aim in this study was to obtain an artificial myocardial patch with a biomimetic cellular organization supported by macroporous tubing in providing medium to the cells in the 3D construct. Initially the WJ MSCs were seeded on Type I collagen coated-mats of PPG2 (3.5 × 6 cm^2) and cultured for 14 days in the CO_2 incubator, to obtain sheets of cells where the cells are aligned parallel to and in contact with each other, as in the native tissue. Confocal microscopy revealed that both the cell bodies and the nuclei were aligned in the direction of the fibers (Fig. 6a).

In the cross section, the cells penetrated effectively into the mat through the interstices between the fibers and occupied the whole thickness (Fig. 6b). The nuclei in the cross section showed that at least 8–9 cell layers could be achieved with the mat used.

Extensive cell growth on the thin mats caused visible mat retraction, in cases when the structure was not strained. This is a positive outcome, since cardiomyocytes need to retract on the surface they adhere to for normal contraction, and this outcome shows that the mats are flexible enough for physical retraction.

3.6. In vitro culture of the 3D construct

Two 3D constructs (construct dimensions: 2 mm height, 4 mm width, 3.5 cm length) were obtained, one for the static and the other for the perfused culture. At the end of the 14-day culture period, the 3D constructs were cut into 1-cm long pieces and used for detection of

cardiomyogenic gene expression via RT-PCR and immunostaining for cardiac specific proteins and determination of cell distribution after cryosectioning.

RT-PCR analysis revealed the expression of the principal cardiac transcription factor Nkx 2.5 and expression of the other cardiac related genes Tbx 5, FOG 2, MEF 2A, MEF 2C and MEF 2D by the cells cultured under both the static and the perfused conditions; this was expected as both the systems had received the same differentiation media (Fig. 7). Under perfused conditions, however, FOG 2 and MEF 2D expression was significantly higher, as evidenced by the intensely stained gel bands. GATA4 expression, however, could be detected in neither of them. Control media contained all experimental media components except the growth factors used for differentiation (valproic acid, insulin and IL 1β) and the cells in this culture expressed neither GATA4 nor Nkx 2.5.

Longitudinal sections (20 μm thick) of the 3D constructs from static and perfused cultures were obtained through cryosectioning and stained with FITC-Phalloidin (Fig. 8) to study the cell distribution and alignment within the structure which is composed of 9–10 layers of aligned fiber mats, with a total thickness of ca. 2 mm. It was observed that in static culture the cells on the outermost layer constituted a viable continuous cell sheet, but a very low cell density was observed at the inner layers (Fig. 8b). The outermost layer had a very high cell density, suggesting cell migration from the inner layers. On the other hand, cell distribution in the mats incubated in the perfused culture was distinctly more homogeneous, and more strikingly there was a cell layer formed around the tubing-mat interface (Fig. 8c). These images confirmed the significant effect of providing nutrients both from inside and outside the 3D structure on maintaining viability and homogeneous distribution. Alignment of cells parallel to fiber direction was maintained within the structure.

Immunostaining for ventricular myosin heavy chain revealed negative results for cells in both cultures. Although expression of major cardiac transcription factors, except GATA4, by these cells was shown, formation of contractile machinery, that is sarcomeres, could not be induced. This outcome points out to the importance of conducting immunocytochemistry besides RT-PCR when an investigation of differentiation to a particular cell lineage is carried out.

4. Discussion

Perfusion of medium via macroporous tubing to multilayered aligned fiber mats significantly increased the viability of mesenchymal stem cells and helped them maintain their anisotropy, thus improving the chances of obtaining viable, thick myocardial patches. The fluorescence images of thin sections of 3D constructs from static and perfused cultures were strikingly different attesting to the positive effect of efficient medium distribution within the 3D structures. Although the cellular penetration within the 15 μm thick single layer mats was very uniform under static conditions, homogeneous live cell distribution in a ca. 2 mm thick and 4 mm wide multilayered 3D construct was not possible without a perfusion system. Comparison of the fluorescence images of sections of 3D constructs from static culture and those from perfused culture revealed that cells can freely move among the fibers. The presence of low numbers of alive cells, distinguished as having a well aligned

actin cytoskeleton, the absence of dead cells in the depths of the mat and the high number of cells on the outer rim in the static culture indicated that the cells have migrated from the inner layers to the surface (Fig. 6a). Normally, due to the dense packing of nanofibers and relatively small pore (or gap) size, cell ingress into nanofibrous meshes is limited to the periphery of thick scaffolds [20,7]. Another reason could be that cell migration toward the inside was discouraged, since nutrient delivery and waste removal are processes driven primarily by diffusion *in vitro* and occur less efficiently in the central regions of the scaffold than at the periphery (facing the medium). Several approaches were reported to improve cellular ingress into thick electrospun scaffolds with small pore sizes [12,21]. The microintegration method was developed by Stankus et al. [21], where simultaneous electrospraying of cells and electrospinning of poly(ester urethane)urea (PEUU) was utilized in order to fabricate thicker (300–500 μm) constructs with more uniform cell incorporation for use in cardiovascular tissue engineering applications. Smooth muscle cell-microintegrated PEUU was strong, flexible and anisotropic, and Trypan blue staining revealed no significant decrease in cell viability as a result of the fabrication process, although the possible effects of exposure to remaining polymer solvent and the conditions necessary for sterility maintenance need to be considered especially during thick scaffold preparations which may take several hours. Nerurkar et al. [12] applied a transient dynamic culture to mesenchymal stem cells seeded on aligned nanofibrous mesh of approximately 0.75 mm thickness by incubating constructs on an orbital shaker; the transient dynamic (6 weeks dynamic followed by 6 weeks static) culture significantly enhanced cell infiltration while permitting glycosaminoglycan and collagen deposition. Taking in account the long time (at least 6 weeks under a dynamic condition) required to provide a uniform cell penetration within only a 0.75 mm thickness, our approach, a uniform penetration to 15 μm-thick single layers within 2 weeks followed by stacking single layers for uniform distribution, offers an attractive alternative to generate thick constructs in a short time.

Poly(glycerol sebacate) prepolymer, which had a low molecular weight and –OH groups in its structure, was introduced into the PHBV:P(L-D,L)LA (1:1) blend to augment its hydrophilicity and elasticity through a plasticizing effect. Type I collagen was adsorbed on the mats to improve cell attachment and increase the probability of cell differentiation through mimicking the native cardiac ECM. Better cell attachment was obtained on PPG mats containing 2 or 4% PGS than 1% PGS. PPG2 mats were chosen to be used in the 3D myocardial construct since the presence of 4% PGS in the blend caused fiber fusions in the mats that would interfere with uniform cell penetration into the structure. PPG2 mats promoted significantly better cell proliferation than PP mats. However, presence of a minor amount (2%) of PGS in the blend caused an increase in the modulus of elasticity, in contrast to our expectations. It was shown by a study by Chen et al. [22] that the concentration of a surfactant plays a critical role in the acquired mechanical properties of a blend. Addition of 2% surfactant to a 1:1 blend of PLLA:PDLLA resulted in a significant increase in storage modulus, while only one percent increase (3% surfactant) resulted in a blend with significantly reduced storage modulus in comparison to a 1:1 blend of PLLA:PDLLA with no surfactant [22]. This sharp difference was attributed to the “bridge” role of the surfactant; at optimum concentration (2%), the surfactant was able to improve the miscibility in the blend. In our study, 2% PGS reinforced the blend as it is evident from the slight increase in

the T_g, and from the increase in the storage modulus. A tension was applied to the mats in the direction of alignment of the fibers. Better fiber alignment was obtained upon use of PGS in the blend, which may have contributed, too, to the increase in the storage modulus [6]. The WJ MSCs, on the other hand, were able to retract the non strained PPG2 mats in the culture, in contrast to what would be expected from a material with such a high storage modulus. Additional investigation, including testing blends with different PGS contents for their mechanical behavior especially at wet state, is required to conclude on the suitability of the PHBV:P(L-D,L)LA:PGS blends for cardiovascular applications.

The best stem cell type with optimal safety for functional engraftment in cardiovascular pathology remains unclear. An intermediate cardiac precommitted phenotype expressing some of the key proteins of a mature cardiomyocyte was proposed for better integration into the cardiac environment [23]. The predifferentiated cells would receive signals from the implantation site and thus achieve a gradual but complete differentiation. In cell transplantation, survival and engraftment within the inflammatory environment of the ischemic myocardium and in the fibrotic scar tissue represent a serious challenge for all types of cells, and more than 90% of the cells in the injected suspension are usually lost [24]. To circumvent these issues, an alternative strategy is to embed the cells in a 3-dimensional structure mimicking the extracellular matrix. The combination of predifferentiated cells with a functionalized scaffold that will promote homing, survival, and function, could be an exciting approach that might prevent ventricular remodeling and improve tissue restoration [23].

Mesenchymal stem cells derived from Wharton's Jelly were used in this study as the cellular component of the potential myocardial patch, considering their properties such as cardioprotective (HGF) and angiogenic (PDGF-B, VEGF) cytokine production [25,26] and differentiation to cardiac cells [27]. WJ MSCs were shown to not express the major histocompatibility complex (MHC) class II (HLADR) antigens [25,28], and were not rejected 4 months after transplantation as xenografts even in the absence of immune suppression, suggesting that they are a favorable cell source for transplantation [28,29]. In previous studies, Wharton's Jelly MSCs were investigated for their potential to differentiate into cardiomyocytes in the presence of 5-azacytidine or in cardiomyocyte-conditioned medium; both treatments resulted in expression of the cardiomyocyte markers N-cadherin, cardiac troponin I, connexin 43, α-actinin, and desmin [30]. Wu et al. [27] investigated the therapeutic potential of WJ MSCs (named as humanumbilical cord derived stem(UCDS) cells in the study) in a rat myocardial infarction model, and statistically significant improvement of cardiac function was observed. Some of the WJ MSCs expressed cardiac troponin-T, von Willebrand factor, and smooth muscle actin, indicating regeneration of damaged myocardium by cardiomyocytic, endothelial, and smooth muscle differentiation. The capillary and arteriole densities were also markedly increased.

A potential cardiomyogenic medium, containing insulin, IL 1β and valproic acid, was used in this study to promote differentiation of WJ MSCs *in vitro*. Activation of the insulin receptor (IR)/IGFR family by insulin and IGF leads to the activation of a signal transduction pathway implicated in the expression of a number of cardiac specific transcription factors such as the zinc finger GATA proteins and Nkx 2.5, which are essential for heart

development [31]. Insulin is also known to act as a cardioprotectant in ischemic/reperfused heart [32]. Histone deacetylases (HDACs) compact chromatin structure and play an important role in global gene expression. Karamboulas et al. [33] showed that HDACs play a repressive role during the entry of mesoderm cells into the cardiac-muscle lineage and that blocking HDAC activity is sufficient to enhance the early stage of cardiomyogenesis. Valproic acid, a HDAC inhibitor, was used in our cardiomyogenic media to investigate its effect in cardiac differentiation. IL 1β is a proinflammatory cytokine that is shown to lead to hypertrophy (increased contractility) in cardiomyocytes by increasing expression of genes encoding the contractile protein MHC, and causes an approximately two fold increase in cell size [34]. It is also involved in prevention of cell apoptosis. Unfortunately no significant promotion of cardiomyogenic phenotype was observed in WJ MSCs when the potential cardiomyogenic media containing the aforementioned factors was used. The only improvement observed was expression of the principal cardiomyogenic gene Nkx 2.5, but formation of a sarcomeric structure could not be induced. However, if differentiation pathways of WJ MSCs to cardiomyogenic lineage are elucidated, the perfusion system developed in this study will lead to cell survival, uniform distribution and maintenance of structural integrity during the differentiation period, which would take two weeks on average.

A recent study reported upregulation in the expression of cardiomyogenesis associated genes in human bone marrow MSCs upon alignment and elongation on fibronectin printed lanes, without any use of soluble differentiation factors [3]. The single comparative study carried out on cardiomyocyte function on electrospun random and aligned polymer fibers showed that cellular alignment enhances cardiomyocyte maturation; cells grown on aligned electrospun polyurethanes had significantly lower steady state levels of atrial natriuretic peptide (ANP) compared to cardiomyocytes on random fibers [8]. In addition to that, Black et al. [35] demonstrated that aligned neonatal rat cardiac cells in fibrin gel generated significantly higher twitch force in comparison to cells at isotropic configuration. Therefore, better healing of cardiac tissue and its functional recovery are expected as a result of the alignment achieved in this study. Our construct provides a means for extensive elongation of WJ MSCs on the structure, and allows cellular integration into a syncytium like organization, both of which are important structural components to be considered to obtain a unified forceful contraction. Therefore, the *in vivo* performance investigation of the 3D myocardial patch developed in this study should be carried out to reveal its potential to be used in improvement of cardiac function with its application on the scarred area following a myocardial infarction.

As a well known phenomenon, if the distance of a cell to a capillary is more than 200 μm then this cell cannot survive due to oxygen and nutrient diffusion limitations [36]. Keeping this principle in mind, 10 layers of mats, each 20 μm thick, were wrapped around one tubing. Having two such units side by side, two tubes surrounded by 10 layers of mats wrapped together, enabled us to have a broader construct. The tubing also served as a supporting component in obtaining closely packed fiber sheets (Fig. 4). The final construct, with the 2 tubes, was 4 mm wide, 2 mm tall and 3.5 cm long. The dimensions of the construct could be arranged by changing the number of mat layers. SEM of the sections of

the 3D construct showed that the mat thickness was 20 μm and the interlayer distance ca. 20 μm. So in this construct, 10 layers of mat with 20 μm mat thickness and a 20 μm spacing among layers around one tubing constituted a 400 μm thick structure with the cells in the mid layers being not further than 200 μm to a nutrition source. The logic of this design is supported by a previous study where Stankus et al. [21] reported on the need for perfusion of 300–500 μm thick aligned fiber scaffolds to maintain a well spread cellular morphology and to promote cell proliferation.

For a clinically relevant result, the thickness of the patch should be close to physiological cardiac-muscle wall thickness which is ca. 6 mm for humans. *In vitro* formation of primitive capillary structures may not be efficient in providing immediate blood circulation to such large engineered tissue grafts *in vivo* [37]. After obtaining an endothelial cell layer in its lumen and ensuring a proper inner diameter and mechanical strength, the macroporous structure that is incorporated into the 3D myocardial construct in this study may serve as a vasculature to enable surgical anastomoses to the coronary arteries, to provide sufficient blood flow to the region. Our future work will be directed toward improvement of this 3D construct and the perfusion system on the way to obtain a more clinically relevant myocardial patch.

5. Conclusion

A method was developed in this study to obtain a thick myocardial patch with a potential to mimic the structure of the native myocardium. Stacking the single layer aligned fiber mats occupied by cells on top of each other would decrease the time necessary to obtain a patch with similar thickness through methods promoting cell penetration. Incorporation of macroporous tubing for nutrient provision within the 3D construct proved to be an efficient way to maintain cell viability, uniform cell distribution and alignment, and may serve as a vasculature to enable surgical anastomoses to the coronary arteries upon improvement. This study represents an important step toward obtaining a thick autologous myocardial patch for ventricular restorations.

Acknowledgments

The authors gratefully acknowledge Prof. Dr. Y. Güngen and Mr. O. Erişöz (Genel Patoloji Merkezi Ltd., Ankara) for the cryosections of the construct, and METU Central Laboratory for the DMA of the mats. This study was supported by EU FP6 Network of Excellence project EXPERTISSUES, and TUBITAK BIDEB Integrated PhD Program (BDP).

References

1. Engler AJ, Sen S, Sweeney HL, Discher DE. Matrix elasticity directs stem cell lineage specification. Cell. 2006; 126(4):677–689. [PubMed: 16923388]
2. Kenar H, Köse GT, Hasirci V. Tissue engineering of bone on micropatterned biodegradable polyester films. Biomaterials. 2006; 27(6):885–895. [PubMed: 16143391]
3. Tay CY, Yu H, Pal M, Leong WS, Tan NS, Ng KW, et al. Micropatterned matrix directs differentiation of human mesenchymal stem cells towards myocardial lineage. Exp Cell Res. 2010; 316(7):1159–1168. [PubMed: 20156435]

4. Park H, Cannizzaro C, Vunjak-Novakovic G, Langer R, Vacanti CA, Farokhzad OC. Nanofabrication and microfabrication of functional materials for tissue engineering. Tissue Eng. 2007; 13(8):1867–1877. [PubMed: 17518744]
5. Godier AF, Marolt D, Gerecht S, Tajnsek U, Martens TP, Vunjak-Novakovic G. Engineered microenvironments for human stem cells. Birth Defects Res C Embryo Today. 2008; 84(4):335–347. [PubMed: 19067427]
6. Mauck RL, Baker BM, Nerurkar NL, Burdick JA, Li WJ, Tuan RS, et al. Engineering on the straight and narrow: the mechanics of nanofibrous assemblies for fiber-reinforced tissue regeneration. Tissue Eng Part B Rev. 2009; 15(2):171–193. [PubMed: 19207040]
7. Baker BM, Mauck RL. The effect of nanofiber alignment on the maturation of engineered meniscus constructs. Biomaterials. 2007; 28:1967–1977. [PubMed: 17250888]
8. Rockwood DN, Akins RE Jr, Parrag IC, Woodhouse KA, Rabolt JF. Culture on electrospun polyurethane scaffolds decreases atrial natriuretic peptide expression by cardiomyocytes in vitro. Biomaterials. 2008; 29:4783–4791. [PubMed: 18823659]
9. Zong X, Bien H, Chung C-Y, Yin L, Fang D, Hsiao BS, et al. Electrospun fine-textured scaffolds for heart tissue constructs. Biomaterials. 2005; 26:5330–5338. [PubMed: 15814131]
10. Evans HJ, Sweet JK, Price RL, Yost M, Goodwin RL. Novel 3D culture system for study of cardiac myocyte development. Am J Physiol Heart Circ Physiol. 2003; 285:H570–H578. [PubMed: 12730055]
11. Radisic M, Euloth M, Yang L, Langer R, Freed LE, Vunjak-Novakovic G. High density seeding of myocyte cells for tissue engineering. Biotechnol Bioeng. 2003; 82:403–414. [PubMed: 12632397]
12. Nerurkar NL, Sen S, Baker BM, Elliott DM, Mauck RL. Dynamic culture enhances stem cell infiltration and modulates extracellular matrix production on aligned electrospun nanofibrous scaffolds. Acta Biomater. 2011; 7(2):485–491. [PubMed: 20728589]
13. Radisic M, Yang L, Boublik J, Cohen RJ, Langer R, Freed LE, et al. Medium perfusion enables engineering of compact and contractile cardiac tissue. Am J Physiol Heart Circ Physiol. 2004; 286(2):H507–H516. [PubMed: 14551059]
14. Kofidis T, Lenz A, Boublik J, Akhyari P, Wachsmann B, Mueller-Stahl K, et al. Pulsatile perfusion and cardiomyocyte viability in a solid three-dimensional matrix. Biomaterials. 2003; 24(27):5009–5014. [PubMed: 14559014]
15. Radisic M, Park H, Chen F, Salazar-Lazzaro JE, Wang Y, Dennis R, et al. Biomimetic approach to cardiac tissue engineering: oxygen carriers and channeled scaffolds. Tissue Eng. 2006; 12(8): 2077–2091. [PubMed: 16968150]
16. Freed LE, Guilak F, Guo XE, Gray ML, Tranquillo R, Holmes JW, et al. Advanced tools for tissue engineering: scaffolds, bioreactors, and signaling. Tissue Eng. 2006; 12(12):3285–3305. [PubMed: 17518670]
17. Kenar H, Kose GT, Hasirci V. Design of a 3D aligned myocardial tissue construct from biodegradable polyesters. J Mater Sci Mater Med. 2010; 21(3):989–997. [PubMed: 19862604]
18. Wang Y, Ameer GA, Sheppard BJ, Langer R. A tough biodegradable elastomer. Nat Biotechnol. 2002; 20(6):602–606. [PubMed: 12042865]
19. Kim B-S, Mooney DJ. Development of biocompatible synthetic extracellular matrices for tissue engineering. TIBTECH. 1998; 16:224–230.
20. Pham QP, Sharma U, Mikos AG. Electrospun poly(epsilon-caprolactone) microfiber and multilayer nanofiber/microfiber scaffolds: characterization of scaffolds and measurement of cellular infiltration. Biomacromolecules. 2006; 7(10):2796–2805. [PubMed: 17025355]
21. Stankus JJ, Guan J, Fujimoto K, Wagner WR. Microintegrating smooth muscle cells into a biodegradable, elastomeric fiber matrix. Biomaterials. 2006; 27:735–744. [PubMed: 16095685]
22. Chen CC, Chueh JY, Tseng H, Huang HM, Lee SY. Preparation and characterization of biodegradable PLA polymeric blends. Biomaterials. 2003; 24(7):1167–1173. [PubMed: 12527257]
23. Spadaccio C, Chachques E, Chello M, Covino E, Chachques JC, Genovese J. Predifferentiated adult stem cells and matrices for cardiac cell therapy. Asian Cardiovasc Thorac Ann. 2010; 18(1): 79–87. [PubMed: 20124305]
24. Zammaretti P, Jaconi M. Cardiac tissue engineering: regeneration of the wounded heart. Curr Opin Biotechnol. 2004; 15:430–434. [PubMed: 15464373]

25. Weiss ML, Medicetty S, Bledsoe AR, Rachakatla RS, Choi M, Merchav S, et al. Human umbilical cord matrix stem cells: preliminary characterization and effect of transplantation in a Rodent model of Parkinson's disease. Stem Cells. 2006; 24:781–792. [PubMed: 16223852]
26. Friedman R, Betancur M, Boissel L, Tuncer H, Cetrulo C, Klingemann H. Umbilical cord mesenchymal stem cells: adjuvants for human cell transplantation. Biol Blood Marrow Transplant. 2007; 13(12):1477–1486. [PubMed: 18022578]
27. Wu KH, Zhou B, Yu CT, Cui B, Lu SH, Han ZC, et al. Therapeutic potential of human umbilical cord derived stem cells in a rat myocardial infarction model. Ann Thorac Surg. 2007; 83(4):1491–1498. [PubMed: 17383364]
28. Medicetty S, Bledsoe AR, Fahrenholtz CB, Troyer D, Weiss ML. Transplantation of pig stem cells into rat brain: proliferation during the first 8 weeks. Exp Neurol. 2004; 190:32–41. [PubMed: 15473978]
29. Fu YS, Cheng YC, Lin MY, Cheng H, Chu PM, Chou SC, et al. Conversion of human umbilical cord mesenchymal stem cells in Wharton's jelly to dopaminergic neurons in vitro: potential therapeutic application for parkinsonism. Stem Cells. 2006; 24:115–124. [PubMed: 16099997]
30. Wang HS, Hung SC, Peng ST, Huang CC, Wei HM, Guo YJ, et al. Mesenchymal stem cells in the Wharton's Jelly of the human umbilical cord. Stem Cells. 2004; 22(7):1330–1337. [PubMed: 15579650]
31. Sachinidis A, Kolossov E, Fleischmann BK, Hescheler J. Generation of cardiomyocytes from Embryonic stem cells. Herz. 2002; 27:589–597. [PubMed: 12439631]
32. Yu QJ, Si R, Zhou N, Zhang HF, Guo WY, Wang HC, et al. Insulin inhibits beta-adrenergic action in ischemic/reperfused heart: a novel mechanism of insulin in cardioprotection. Apoptosis. 2008; 13(2):305–317. [PubMed: 18165901]
33. Karamboulas C, Swedani A, Ward C, Al-Madhoun AS, Wilton S, Boisvenue S, et al. HDAC activity regulates entry of mesoderm cells into the cardiac muscle lineage. J Cell Sci. 2006; 119(20):4305–4314. [PubMed: 17038545]
34. Petersen CA, Burleigh BA. Role for Interleukin-1β in Trypanosoma cruzi-induced cardiomyocyte hypertrophy. Infect Immun. 2003; 71(8):4441–4447. [PubMed: 12874323]
35. Black LD 3rd, Meyers JD, Weinbaum JS, Shvelidze YA, Tranquillo RT. Cell-induced alignment augments twitch force in fibrin gel-based engineered myocardium via gap junction modification. Tissue Eng Part A. 2009; 15(10):3099–3108. [PubMed: 19338433]
36. Morritt AN, Bortolotto SK, Dilley RJ, Han X, Kompa AR, McCombe D, et al. Cardiac tissue engineering in an in vivo vascularized chamber. Circulation. 2007; 115:353–360. [PubMed: 17200440]
37. Zimmermann WH, Cesnjevar R. Cardiac tissue engineering: implications for pediatric heart. Pediatr Cardiol. 2009; 30:716–723. [PubMed: 19319461]

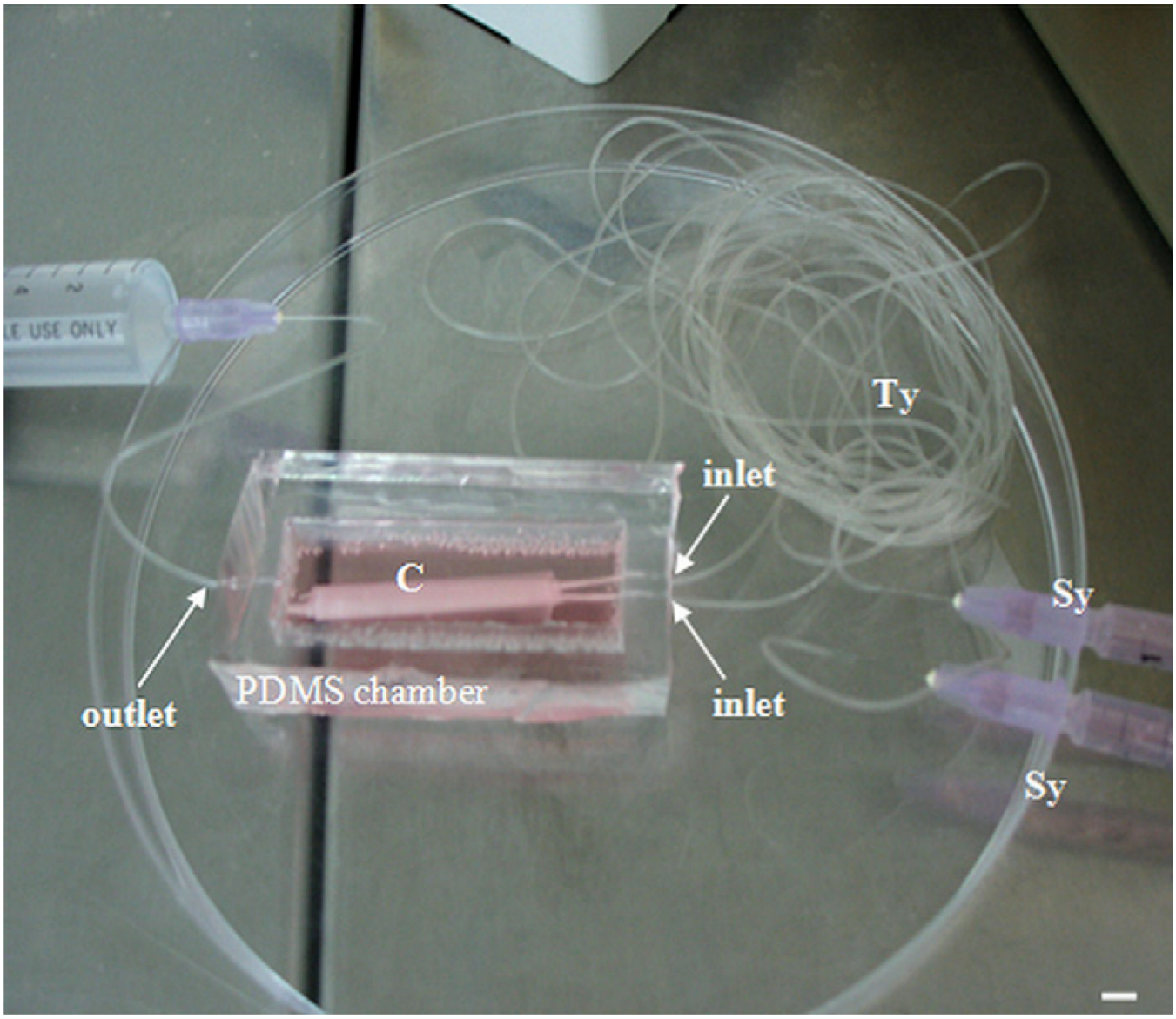

Fig. 1.

The perfused 3D construct (C). The two 1 mL syringes (Sy) on the right are used to deliver cell growth media through the Tygon tubes (Ty) to the two inlets of the PDMS chamber and the medium continues to flow through the nonporous parts of the biodegradable tubes inserted at the inner holes of the inlets. Finally the medium is delivered to the cells in the mats by diffusing through the walls of macroporous portion of the tubes that are wrapped by the mats. The end of the Tygon tubing residing at the outlet of the chamber (occupied by another big syringe full of fluid) is opened during the medium perfusion process, to allow the outflow of excess fluid from the PDMS chamber. Scale bar: 4 mm.

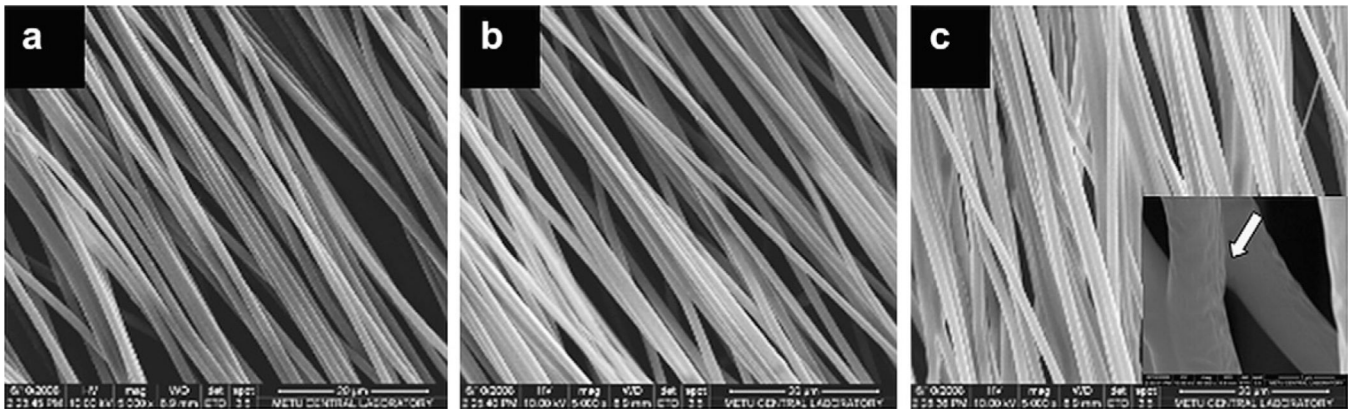

Fig. 2.

Electrospun PHBV:P(L-D,L)LA (1:1) with a) 1%, b) 2% and c) 4% w/w PGS in Chl:DMF (95:5). Magnification: ×5,000. The white arrow in the inset points out a fiber fusion.

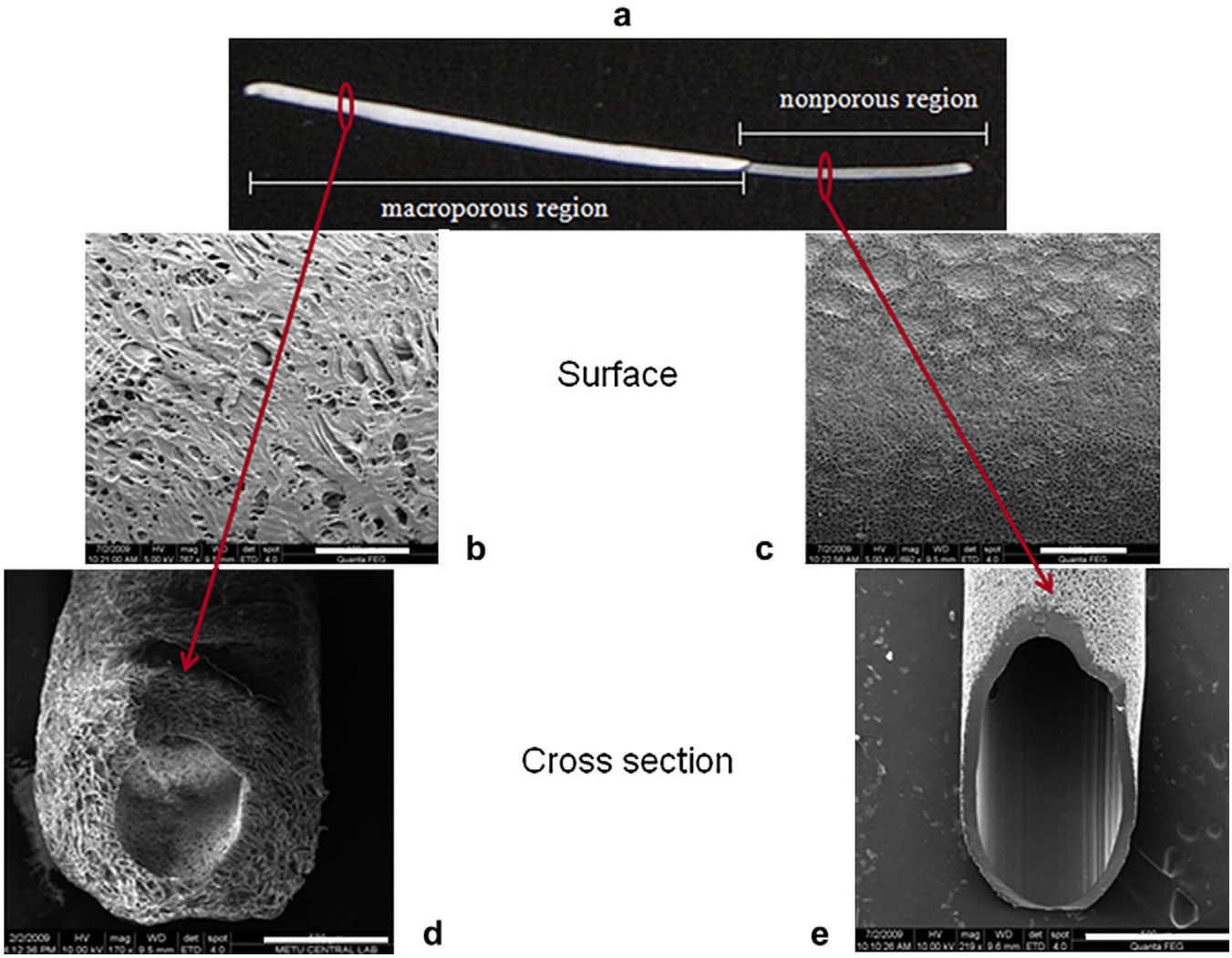

Fig. 3.

Stereomicroscope and SEM images of a bifunctional P(L-D,L)LA:PGS (96:4) tubing: a) stereomicrograph showing the whole tube, b and d) surface and cross section of the macroporous region, c and e) surface and cross section of the nonporous region. Scale bars: b, c) 100 μm, d, e) 500 μm.

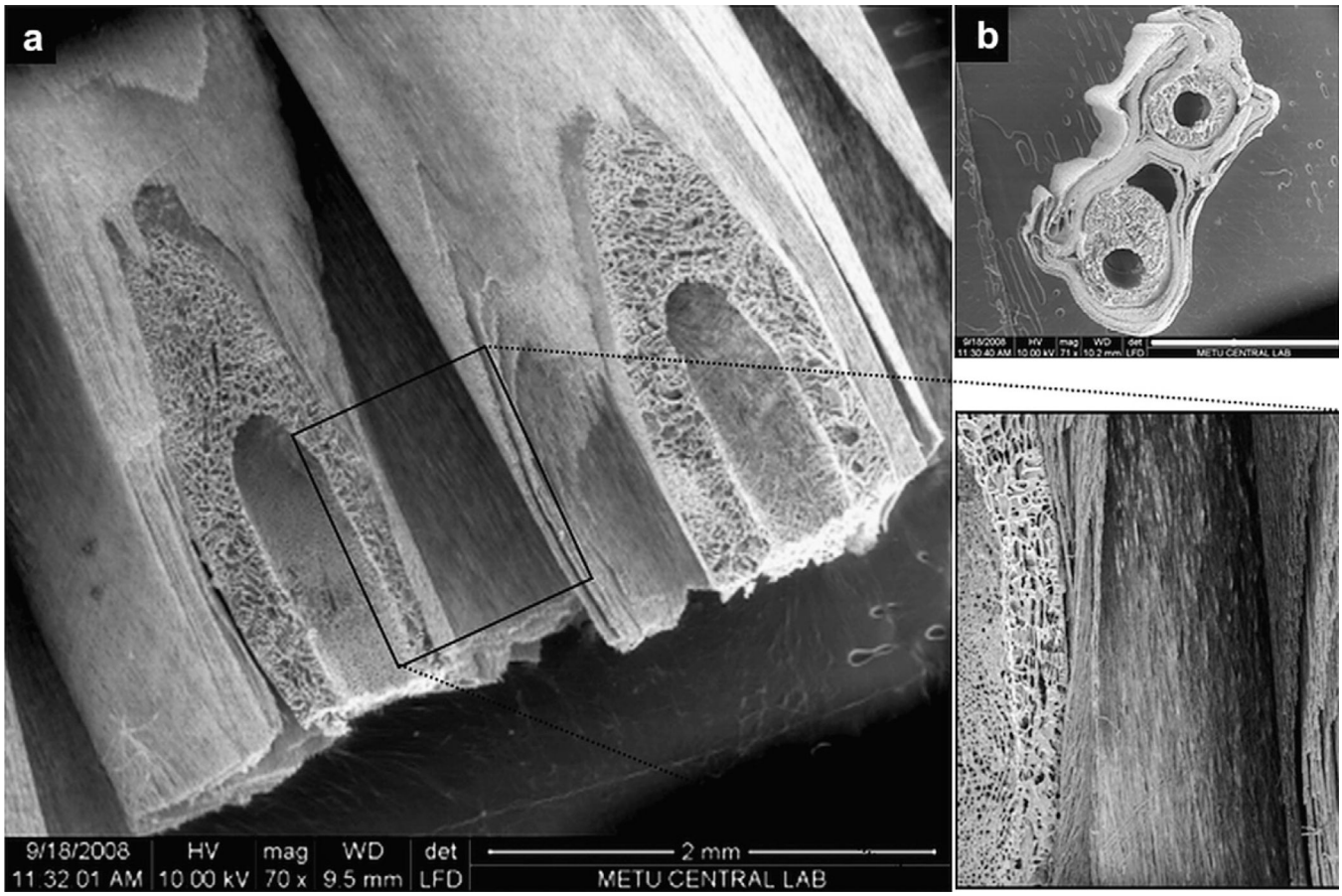

Fig. 4.

SEM images of sections from the 3D construct. a) Diagonal view of the 3D construct showing the parallel arrangement of mat fibers to the longitudinal axis of the tubing and the mat-tubing association, b) Cross section of the 3D construct. Scale bar: 2 mm.

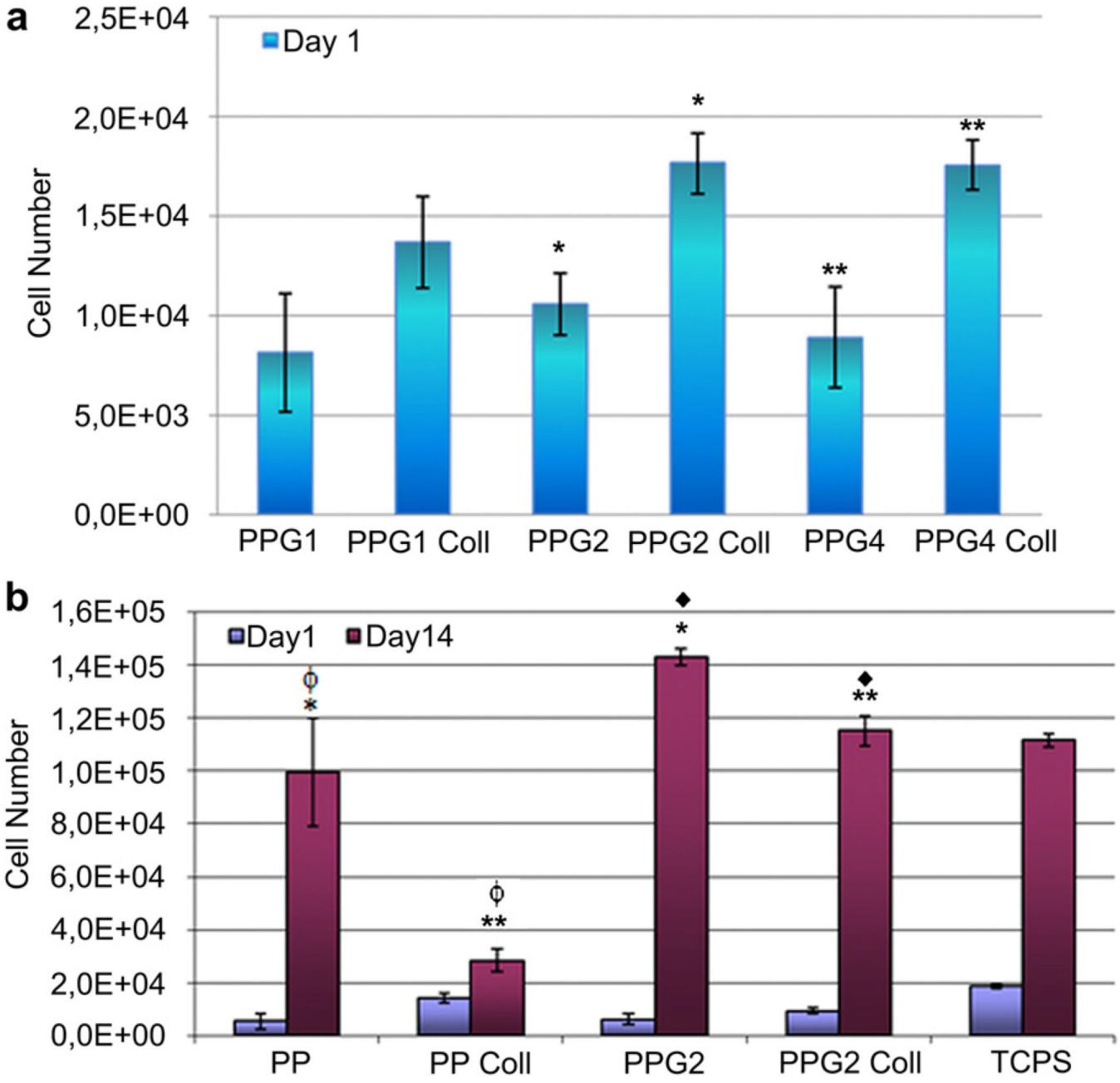

Fig. 5.

hWJ MSC attachment and proliferation on aligned fiber PHBV:P(L-D,L)LA (PP) and PHBV:P(L-D,L)LA:PGS (PPG) mats within 14 days after cell seeding. 1, 2 and 4 represent the percentage of PGS in the blend. Coll: Collagen (adsorbed), TCPS: Tissue culture polystyrene. Data are expressed as mean ± SD. *, **, ◆, φ indicate pairs significantly different from each other ($p < 0.05$).

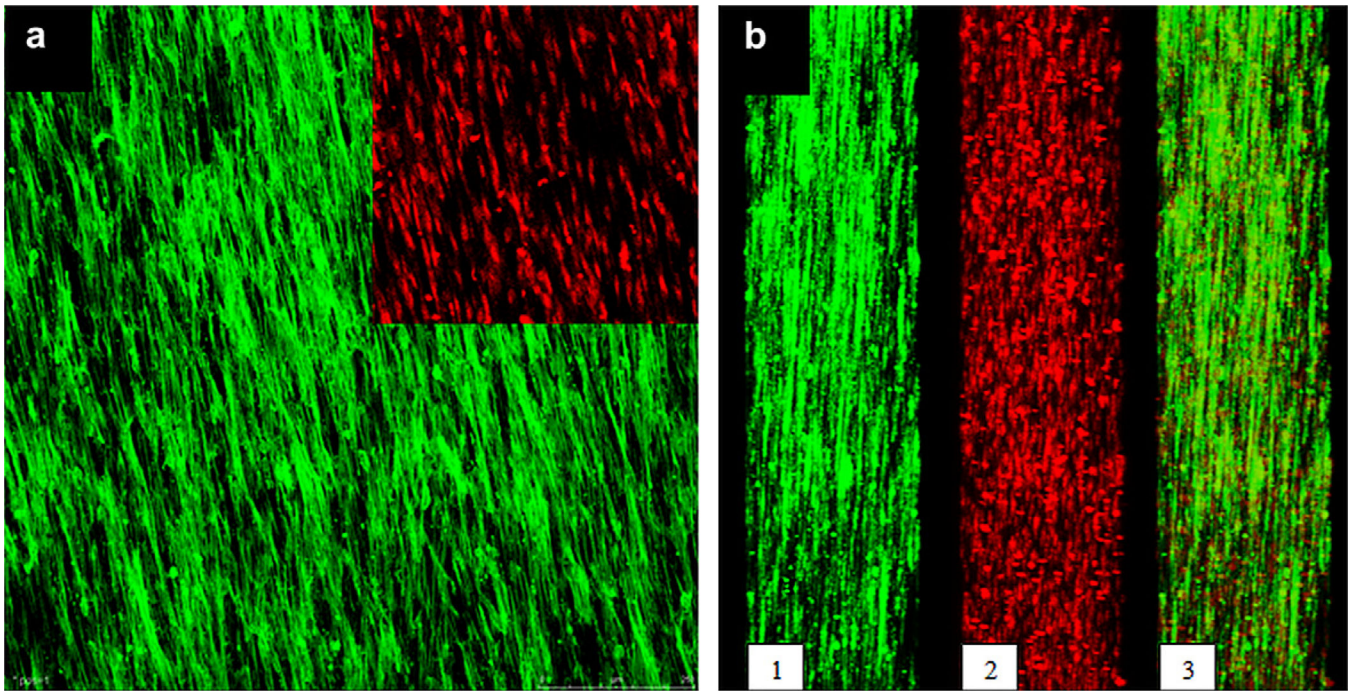

Fig. 6.

The confocal micrographs of WJ MSCs grown for 14 days on aligned fiber PPG2 mats: a) top view (inset shows only the nuclei), b) cross sectional view in *Y* direction: 1- F-actin alignment, 2- nuclear alignment, 3- overlay of 1 and 2. Cells were stained with FITC-Phalloidin and PI (×100). Green: F-actin, red: cell nuclei. Scale bar: 250 μm. (For interpretation of the references to colour in this figure legend, the reader is referred to the web version of this article.)

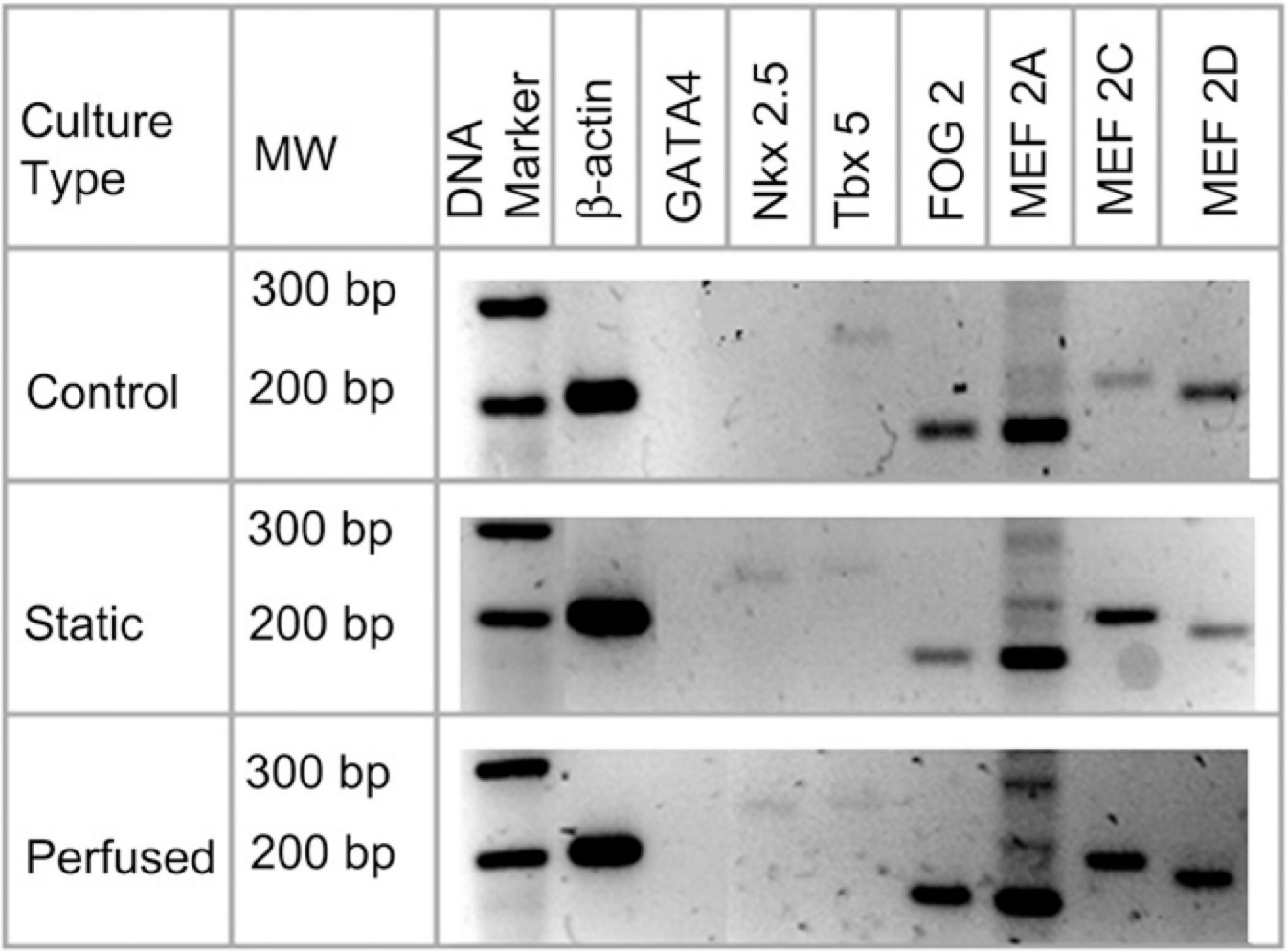

Fig. 7.

Cardiac transcription factor expression by hWJ MSCs cultured in static and perfused cultures. The control represents gene expression of cells cultured on tissue culture polystyrene in media without the differentiation factors (valproic acid, insulin and IL 1β).

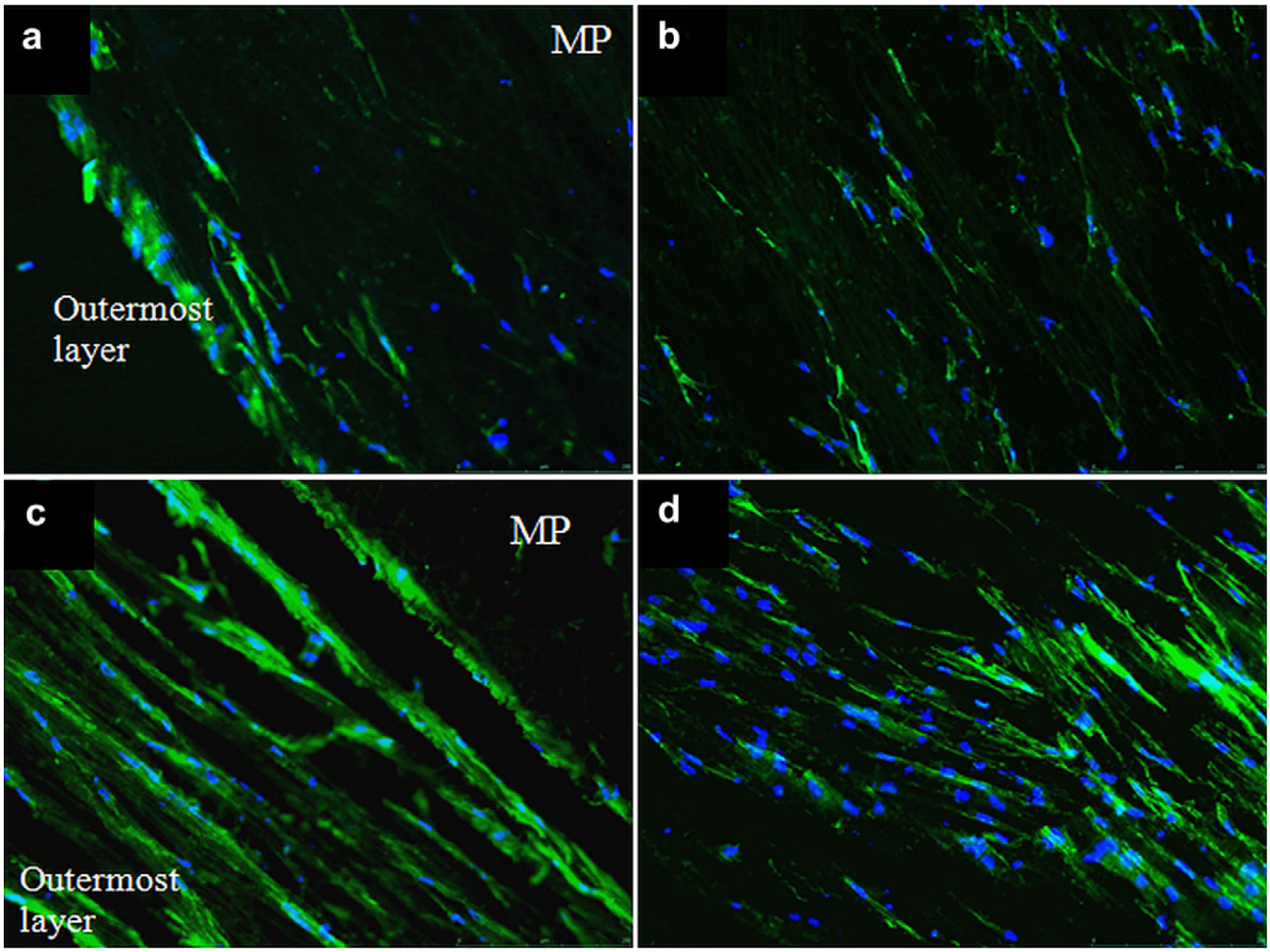

Fig. 8.

Phalloidin and DAPI stained cryosections of the 3D constructs from static (a, b) and perfused cultures (c, d): a and c show the outermost layers (further from the tubes and closest to the medium in the chamber), and b and d show midpoints of the construct cross sections (×10). Green: F-actin, Blue: cell nuclei, MP: macroporous tubing. (For interpretation of the references to colour in this figure legend, the reader is referred to the web version of this article.)

Table 1

Primers used in RT-PCR analysis.

Gene	Primer Sequence (Forward-Reverse)	Product Size (bp)
Housekeeping gene β-Actin	5′-AACGGTGAAGGTGACAGCA-3′	202
	5′-TGTGTGGACTTGGGAGAGG-3′	
GATA binding protein 4 (GATA4)	5′-AACGGAAGCCCAAGAACC–3′	246
	5′-AGAGGACAGGGTGGATGGA–3′	
NK2 transcription factor related, locus 5 (Nkx 2.5)	5′-ATGGTATCCGAGCCTGGTAG-3′	211
	5′-ATAATCGCCGCCACAAAC-3′	
Myocyte enhancer factor 2A (MEF 2A)	5′-CAATGCCGACTGCCTACAA-3′	166
	5′-AACTGCCCTCCAGCAACA-3′	
Myocyte enhancer factor 2C (MEF 2C)	5′-CCAGGCAGCAAGAATACGAT -3′	227
	5′-AACCCAGACAGAGATGACAGGT -3′	
Myocyte enhancer factor 2D (MEF 2D)	5′-GGCAACAGCCTAAACAAGGTC -3′	210
	5′-GGTGGTGAGCGAATGAGTAGA -3′	
T-box 5 (Tbx5)	5′-GCGGATGTTTCCCAGTTACA -3′	253
	5′-CAGGTGGTTGTTGGTGAGC -3′	
Zinc finger protein friend of GATA 2 (FOG 2)	5′-CCAGGCTTCCTCAAATGG-3′	170
	5′-TGTGGTCGTCTTCGTGCT-3′	

Table 2

DMA results of PHBV:P(L-D,L)LA (1:1) (PP) and PHBV:P(L-D,L)LA:PGS (49:49:2) (PPG2) mats.

Mat Type	T(°C)	Storage Modulus (E′) (MPa)			Loss Modulus (E″) (MPa)			Tangent Delta			T_g (°C)					
		1 Hz	2 Hz	4 Hz	1 Hz	2 Hz	4 Hz	1 Hz	2 Hz	4 Hz	1 Hz		2 Hz		4 Hz	
PP	25	258	272	284	24	34	48	0.093	0.124	0.170	54.32		55.99		57.11	
	37	258	275	291	34	44	57	0.132	0.159	0.194						
PPG2	25	528	554	579	44	62	90	0.083	0.111	0.155	−14.37	55.11	−14.37	56.18	−14.99	57.81
	37	480	508	535	54	68	90	0.112	0.134	0.169						